Non-linear Failure Analysis of FRP Laminates composed of UD laminae - A comparison of the author's predictions with test results within the worldwide Failure Exercise in the UK -

R. G. Cuntze

Prof. Dr.-Ing. habil. Ralf Georg Cuntze, MAN Technologie AG , Franz-Josef-Strauß-Str. 5, D-86153 Augsburg, Germany; Tel: 0049 821 505-2593, Fax: -2630, E-mail: *Ralf_Cuntze@mt.man.de*.

Keywords: Failure criteria UD laminae, non-linear behaviour of laminae and laminates, failure of laminates

Abstract: The paper presents the author's contribution to a worldwide exercise on 'Failure theories for fibre-reinforced plastic (FRP) laminates composed of unidirectional (UD) laminae', [1, 2].

An assessment is made of the correlation between predictions and experimental results provided for a couple of test cases involving biaxial initial and final failure envelopes and stress strain curves of various unidirectional and multidirectional laminates. The theory, implemented into a computer code, employs 3D failure criteria for UD laminae together with non-linear modelling of laminae and laminate. The criteria are based on the author's Failure Mode Concept (FMC), which provides a set of failure criteria formulated on lamina level that allows for a prediction of the critical lamina failure mode. The generated computer code captures relatively large laminate strains to failure. Special emphasis has been put on the difference between an isolated and an embedded UD lamina.

The correlation between the predictions and the experimental data is very satisfactory for multiaxially loaded UD laminae, and is generally satisfactory for the laminates, especially where Fibre Failure (FF) is the dominant mode, which is the case for well-designed (according to netting theory) laminates. Discrepancy between predictions and test data was largest for the ±55°-angle ply glass/epoxy laminates that experienced very large deformations usually not permitted in structural practice. To tackle such an extreme test case (TC) would involve post failure progression analysis far beyond the occurrence of the various Inter Fibre Failure (IFF) modes.

There was a lack of UD test data domains in some of the test cases. Furthermore, in some lamina and laminate test cases 'jumping' of experimental data is observed that cannot be explained by scatter. Where possible, a re-evaluation of experimental results was executed which reduced the discrepancy between prediction and experiment very much.

1. Introduction

Composite materials have become increasing application in industries such as aerospace, automotive, mechanical engineering, civil and chemical engineering. Focusing increasing application of composites requires safe design tools. Practical composite failure criteria for UD laminae are amongst these design tools, however it turned out that they should be further improved. As failure of a lamina –utilized as building block of a laminate- does not cover *failure of the laminate*, failure theories are addressed that consist, both, of failure criteria and of nonlinear analysis to consider the degrading lamina behaviour within the laminate.

1.1 The Failure Exercise

Since 1992 a worldwide exercise is underway to monitor and check the current capability of methods for predicting the strength of fibre composite laminates. It was organised at UMIST and QinetiQ, UK, by Prof. Dr. M. J. Hinton, Mr. P. D. Soden and Dr. A. S. Kaddour.

In this exercise (cited from [3]), selected workers were invited to submit papers to a strictly controlled format. A series of laminate configurations, load cases, and input data were defined by the organisers. Test cases were selected to challenge the theories to the full. These test cases include carbon and glass fibres, different epoxy matrices, stacking sequences, and loading conditions invol-

ving uni-axial and bi-axial tension and compression, torsion shear, as well as combinations of them.

As test results, those available from tube specimens were chosen because the simpler coupon specimens are encountered with the free edge effect. Also, a wider range of stress states can be applied to tubes by combinations of internal or external pressure, torsion, and axial load, ([4).
Nevertheless some problems remain: the tubes have to be designed to avoid torsion and compression buckling, failures at the end constraints, and to minimise possible changes in geometry (widening, barrelling). Each tube specimen was tested at a fixed ratio of hoop to axial stresses. Loads were increased monotonically until fracture occurred. Unless otherwise stated the fracture stress states given were calculated based on *un-deformed* tube dimensions with no allowance (usual practice in evaluation) made for change of shape during loading. The ply angle is specified to be 90° for the hoop direction (denoted y).

The various tasks were predictions of: 1.) Bi-axial failure envelopes of the UD Laminae; 2.) Initial and final failure envelopes of the laminates and 3.) The shape of the stress-strain curves of the laminates. The contributors should indicate initial failure, leakage failure (in case of internal pressure) and final fracture.

In Part A of the Failure Exercise, Ref[3], all contributors were given exactly the same set of material properties and were asked to predict in a 'blind' test the multi-axial strength of an associated set of test cases (TC) of laminae and of laminates. In Part B (for the 'post-runners' all results of their Parts A and B will be published in a Part C) at first available experimental results had to be superimposed on the 'blind' theoretical predictions and later, lacks of coincidence were asked for comments by the contributors. By the organisers, the 'blind' predictions of the authors as well as probable later improvements were superimposed ([5, 6]) on top of each other and compared. All papers, both, from contributors and organisers are published in the journal 'Composites Science and Technology'.

1.2 Requirements from Standards

According to some standards, e.g. Ref[7], in any static design, a designer has in general to dimension a laminate against two main types of failure, namely inter-fibre-failure (IFF) of the *laminae* and fibre-failure (FF). Sometimes it might be further required to prove that IFF should not occur if a laminate is subjected to the so-called 'Design Limit Load (DLL)' times a factor of safety j. In practice in case of isotropic materials this corresponds to the Yield *Proof of Design* (is a deformation requirement!). This means for composites: 'No IFF below DYL = DLL* j_{yield}'. For Ultimate *Proof of Design* is valid 'No FF below DUL = DLL* j_{ult}' (is a fracture requirement).
An IFF mode normally indicates the *onset of failure* in a laminate whereas the appearance of a FF mode in a single *lamina* usually marks the *final failure* of the laminate.
In the case of brittle (this material behaviour is addressed here) FRP composites, failure coincides with fracture. Fracture is defined in this article as a separation of material. The material is assumed to be initially free of damage such as technical cracks (size in the order of a mm) and delaminations but not free of tiny defects/flaws (size in the order of microns) prior to loading.

1.3 Failure Theory

Modelling the behaviour of materials remains one of the most difficult challenges in engineering. With the development of the FEA codes and of the capacity of the hardware multidimensional analyses have become state-of-the-art. They are becoming affordable even for layered composite structures. This development confronts the designer with the assessment of 3D-states of stress by strength criteria. 'Economic' failure theories are desired that are capable to accurately predict stresses in the laminae of the laminate and to judge these stresses reliably.
A failure theory consists of failure criteria and non-linear analyses. Non-linear analysis itself incorporates non-linear stress-strain behaviour of the lamina and of the laminate.

For design engineers the choice of the macro-mechanical level in modeling is mandatory wrt get-

ting macro-mechanical stresses from numerical analysis. Describing failure by macro-mechanical stresses in general is different to an application of the really failure mechanisms-causing micro-mechanical stresses (see later the IFF1).

2 The Failure Mode Concept (FMC)

2.1 Lamina Stresses, Invariants, and Properties

Figure 1 depicts the 3D state of stress, the 5 strengths, and the 5 elasticity quantities of a UD material element. The lamina is defined here to be the material or the building block that a laminate is made of, see *Fig.2* and [8].

The characterisation of the strength of transversally-isotropic composites requires –according to the FMC- the measurement of five independent basic lamina strengths: $R_{||}^{t}$ *and* $R_{||}^{c}$ (tensile and compression strengths parallel to the fibres); $R_{\perp}^{t}$ *and* $R_{\perp}^{c}$ (tensile strength and compressive strength transversal to the fibre direction); and $R_{\perp||}$ (shear strength transverse/parallel to the fibres. Prior to the FMC the measurement of these *5* strengths still became standard. *Note*: $\overline{R}$ denotes a mean or typical strength value (to be used in *stress analysis*) whereas R is either a general value or the so-called design allowable (to be used in *strength analysis* or *Proof of Design,* resp.).

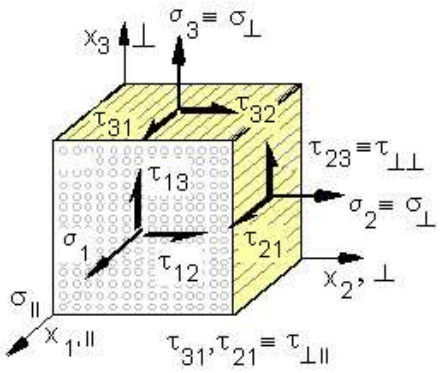

Fig.1: Stresses, invariants and strength notations of a UD lamina. 3D state of stress. [8]
t: = tension, *c*: = compression, *f* := index fibre.

$$R_{||}^{t}(=X^{t}),\ R_{||}^{c}(=X^{c}),\ R_{\perp||}(=S),\ R_{\perp}^{t}(=Y^{t}),\ R_{\perp}^{c}(=Y^{c})\ ,$$

$$E_{||},\ E_{\perp},\ G_{||\perp},\ \nu_{\perp||},\ \nu_{\perp\perp}\ ;\ \{\sigma\}=(\sigma_1,\sigma_2,\sigma_3,\tau_{23},\tau_{13},\tau_{12})^{T},$$

$$I_1=\sigma_1\approx \mathrm{v}_f\,\sigma_{1f}\quad\text{with}\quad \sigma_{1f}=\varepsilon_1\cdot E_{||}/\mathrm{v}_f, \qquad (1)$$

$$I_2=\sigma_2+\sigma_3,\quad I_4=(\sigma_2-\sigma_3)^2+4\tau_{23}^2\ \text{[Boehler]}$$

$$I_4=\tau_{31}^2+\tau_{21}^2,\quad I_5=(\sigma_2-\sigma_3)(\tau_{31}^2-\tau_{21}^2)-4\tau_{23}\tau_{31}\tau_{21}.$$

I_5 considers physical difference of $\tau_{21}(\sigma_2)$ to $\tau_{31}(\sigma_2)$

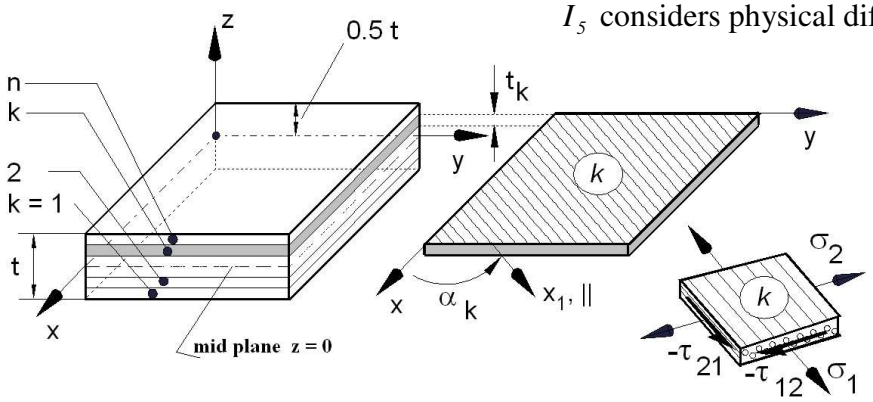

Fig.2: Laminate and k' th lamina subjected to a plane state of stress (mid-plane z = 0)

2.2 FF Modes and IFF Modes

Fractography reveals, see *Fig.3*:

- The total number of modes, see [8], is five; two FF modes and three IFF modes. The IFF modes incorporate cohesive fracture of the matrix and adhesive fracture of the fibre-matrix interface. Both fracture types are often termed 'matrix failure'.
- The 'explosive' effect of the so-called *wedge shape failure* of a lamina in a laminate, which is an IFF mode caused by high transverse stress $\sigma_{\perp}^{c}$, [9, 8], may lead directly to *final failure*, as for example in the case of Puck's torsion spring. It can also lead indirectly to a final failure of a laminate via the development of through thickness stresses and, local delaminations and hence to the wedge buckling of an adjacent compression–loaded lamina. This IFF, where parts of a lamina move in the thickness direction may also initiate a catastrophic failure like FF (*Fig.3*). The

grade of criticality depends on the lay-up: A load-carrying outer hoop layer of a pressure vessel is of highest criticality.

Loading a composite by a $\sigma_{\parallel}$ stress will always induce a matrix stress acting in the fibre direction. The matrix stress is normally obtained from use of micro-mechanics equations, see for instance the appendix in [10]. However, as long as the fracture strain of the matrix is much larger than that of the fibre (eg fibre *2%*, matrix *6%*) one may neglect matrix stresses in the fibre direction of a 0° layer because their magnitude does not practically affect the failure of the fibres.

Fig.4 outlines the criticality of the fracture modes.

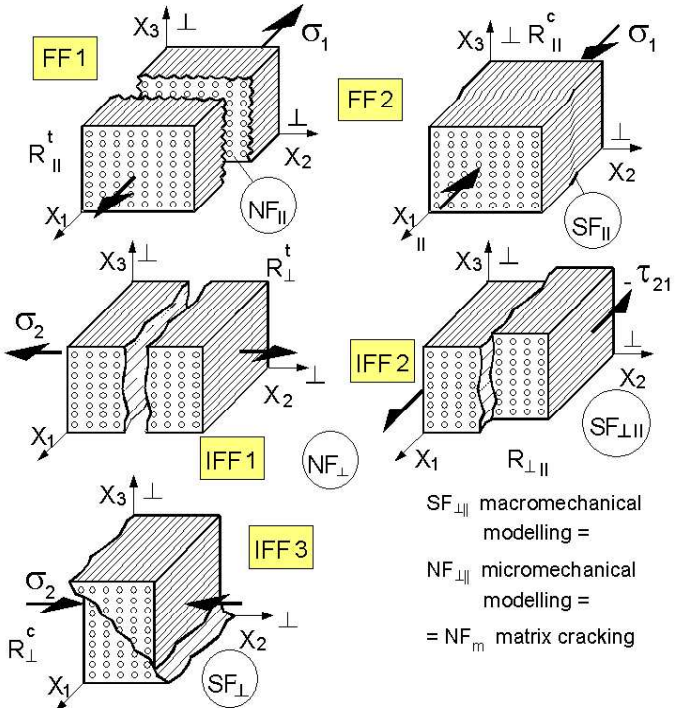

Fig.3: Fracture modes (types) in transversally-isotropic material.
NF:= Normal Fracture,
SF:= Shear Fracture

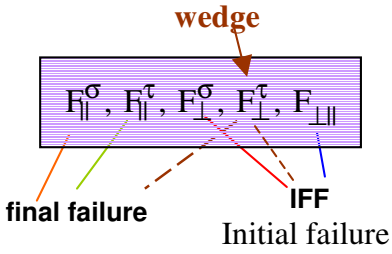

Fig.4: Failure mode criticality

2.2 Establishment of FMC-based 3-dimensional UD Failure Criteria stress interaction

The FMC generates a phenomenological three-dimensional, lamina stress-based *engineering*

Table 1: Main features of the FMC and the non-linear stress analysis

- According to the symmetry of a transversally-isotropic material there are 5 strengths, 5 elasticity quantities and the FMC postulates 5 failure modes
- Each *mode* represents one theoretically independent failure mechanism and one piece of the complete *failure surface* (surface of the multidimensional failure body or so-called *limit surface*)
- Each failure *mechanism* is represented by one failure *condition*. One failure mechanism is governed by one basic strength and therefore has a clearly defined equivalent stress σ_{eq} and stress effort Eff
- Invariant formulations of the failure conditions in order to achieve a *scalar* potential considering the material's symmetries are derivable for each mode. Each invariant term in the failure condition is related to a physical mechanism observed, whether causing a volume change or a shape change (compare Mises in isotropic case), or 'internal friction' in the material element
- Different, however, similar behaving materials obey the same function as failure condition but have *different curve parameters*
- Curve-fitting of the course of test data is only permitted in the pure failure mode's regime
- For each *mode* one stress-based *reserve factor* $f_{Res}^{(mode)}$ (if linear) or one *stress effort* is to be determined, displaying by the lowest (highest risk) mode reserve factor, where the design key has to be turned
- The probabilistics-based 'rounding-off' approach delivers the *resultant reserve factor* linked to the *margin of safety* by $MS = f_{Res}^{(res)} - 1$ necessary for a *Proof of Design*

approach. The occurring fracture failures may be of various types resp. mechanisms (M*ind*: yielding represents just one mechanism).

Cuntze's method of applying the FMC methodology (see *Table 1*) is to propose a set of equations describing five failure modes in each lamina (ply) and then combine these equations in a suitable manner to predict failure in a lamina in order to consider the superposition of *all* failure affecting modes. Each failure mode is described by a distinct equation containing terms showing an ***interaction between*** the various active ***stresses*** *(stress tensor components)*. The method can be easily adapted to finite element (FE) codes by using the FE output stresses as input values in the following set of *failure conditions*, $F(\{\sigma\}) = 1$

$$FF1: \quad F_{\parallel}^{\sigma} = \frac{I_1}{\overline{R}_{\parallel}^{t}} = 1, \qquad FF2: \quad F_{\parallel}^{\tau} = \frac{-I_1}{\overline{R}_{\parallel}^{c}} = 1,$$

$$IFF\ 1: \quad F_{\perp}^{\sigma} = \frac{I_2 + \sqrt{I_4}}{2\overline{R}_{\perp}^{t}} = 1\ , \qquad IFF\ 2: \quad F_{\perp\parallel} = \frac{I_3^{3/2}}{\overline{R}_{\perp\parallel}{}^{3}} + b_{\perp\parallel}\frac{I_2 I_3 - I_5}{\overline{R}_{\perp\parallel}{}^{3}} = 1, \qquad (2a\text{-}2e)$$

$$IFF\ 3: \quad F_{\perp}^{\tau} = (b_{\perp}^{\tau} - 1)\frac{I_2}{\overline{R}_{\perp}^{c}} + \frac{b_{\perp}^{\tau}\sqrt{I_4}}{\overline{R}_{\perp}^{c}} = 1\ .$$

Besides the design-mandatory 5 strengths these contain two *curve parameters* ($b_{\perp\parallel}$, $b_{\perp}^{\tau}$) that are to be determined from multi-axial test data in the associated pure domain or can be estimated by experience. (*Remind:* $F_{\parallel}^{\sigma}$: $I_1 = \sigma_1 = v_f \cdot \sigma_{1f} = v_f \cdot \varepsilon_1 \cdot E_{1f} = \varepsilon_1 \cdot E_{\parallel}$ with σ_{1f} = tensile fibre stress, see[14]). Simplified, one calibration point □ for each mode, see [8], delivers after inserting them into the IFF conditions for $F_{\perp\parallel}$ (from $\left(\sigma_2{}^{c}, \tau_{21}^{\perp\parallel}\right)$ e.g.) and $F_{\perp}^{\tau}$ (from $(\sigma_2^{c\tau}, \sigma_3^{c\tau})$ and after a further resolution

$$b_{\perp\parallel} = \frac{1 - \left(\tau_{21}^{\perp\parallel} / \overline{R}_{\perp\parallel}\right)^2}{2\sigma_2^{c} \cdot \tau_{21}^{\perp\parallel 2} / \overline{R}_{\perp\parallel}^{3}} \qquad \text{and} \qquad b_{\perp}^{\tau} = \frac{1 + (\sigma_2^{c\tau} + \sigma_3^{c\tau}) / \overline{R}_{\perp}^{c}}{(\sigma_2^{c\tau} + \sigma_3^{c\tau}) / \overline{R}_{\perp}^{c} + \sqrt{(\sigma_2^{c\tau} - \sigma_3^{c\tau})^2} / \overline{R}_{\perp}^{c}}\ . \qquad (3a,\ b)$$

Practical safe bounds for GFRP, CFRP and AFRP are $0.05 < b_{\perp\parallel} < 0.15$, $1.0 < b_{\perp}^{\tau} < 1.15$. A value $b_{\perp\parallel} = 0$ means 'no bulge effect', and $b_{\perp}^{\tau} = 1$ means 'no friction' in the $\perp\perp$-plane. If a calibration point for $b_{\perp}^{\tau}$ is still missing, $b_{\perp}^{\tau} = 1$ during pre-dimensioning is recommended as it provides a safe lower bound. Also, during pre-dimensioning the assumption of $b_{\perp\parallel} = 0$ is helpful and simplifies the FMC-based equations to the Tsai/Wu model level, [11]. In non-linear laminate analysis $b_{\perp\parallel} = 0$ might be acceptable. This further avoids the only numerical difficulty, raised by $F_{\perp\parallel\parallel}$, [14].

With regard to the 3D nature of the *lamina* IFF conditions, both, IFF1 ($F_{\perp}^{\sigma}$:= transverse tensile failure, cracking due to inter-laminar stresses $(\sigma_3^{t}, \tau_{32}, \tau_{31})$) and IFF3 ($F_{\perp}^{\tau}$:= wedge failure, the intra-laminar stresses (σ_2^{c}, τ_{21}) cause cracking and a local 3D stress state) may also serve as criteria for the 'onset of delamination' which is termed *laminate* failure.

2.3 Determination of Mode Reserve Factors (allowing for interaction of the lamina stresses)

In the following set of formulae the *reserve factor* of each mode is provided,

$$f^{\parallel\sigma} = \overline{R}_{\parallel}^{t} / (\varepsilon_1 \cdot E_{\parallel}) = R_{\parallel}^{t} / \sigma_{eq}^{\parallel\sigma}, \qquad f^{\parallel\tau} = -\overline{R}_{\parallel}^{c} / \sigma_1 = -\overline{R}_{\parallel}^{c} / \sigma_{eq}^{\parallel\tau}\ , \qquad (4a,\ 4b)$$

$$f^{\perp\sigma} = 2\overline{R}_{\perp}^{t} / [I_2 + \sqrt{I_4}] = \overline{R}_{\perp}^{t} / \sigma_{eq}^{\perp\sigma}\ , \qquad (4c)$$

$$f^{\perp\parallel} = \overline{R}_{\perp\parallel} / [I_3^{3/2} + b_{\perp\parallel}(I_2 I_3 - I_5)]^{1/3} = \overline{R}_{\perp\parallel} / \sigma_{eq}^{\perp\parallel}\ , \qquad (4d)$$

$$f^{\perp\tau} = \overline{R}_{\perp}^{c} / [(b_{\perp}^{\tau} - 1) I_2 + b_{\perp}^{\tau}\sqrt{I_4}] = \overline{R}_{\perp}^{c} / \sigma_{eq}^{\perp\tau}\ , \qquad (4e)$$

according to the general equation $f_{\mathrm{Re}s}^{(\mathrm{mod}e)} = \overline{R}^{\mathrm{mod}e} / \sigma_{eq}^{\mathrm{mod}e}$, together with the so-called *equivalent*

stress. An equivalent stress includes all load stresses and residual stresses that are acting together in a given mode.

2.4 Interaction of Failure Modes or Determination of Resultant Reserve Factors

Mechanical and probabilistic interactions cannot be clearly distinguished and therefore, the author models the failure mode interactions by a simple probabilistic-based 'series spring model' approach [12, 13], that is a so-called 'logical model of the lamina failure system'. By this method, the *interaction between* FF and IFF *modes* as well as between the various IFF modes acts as a rounding-off procedure linked to the determination of the desired values for the most often stress-based $f_{\mathrm{Re}s}^{(res)}$ or for $Eff^{(res)}$ (then, just in linear case $Eff^{(res)} = 1/f_{\mathrm{Re}s}^{(res)}$). In these so-called Mixed Failure Domains MiFD, the desired *(resultant) Reserve Factor* $f_{\mathrm{Re}s}^{(res)}$ takes automatically into account the interactions between all the various modes (in non-linear case the formulation has to be load-based, that is the exact one) utilizing the formula

$$(1/f_{\mathrm{Re}s}^{(res)})^{\dot{m}} = f(f_{Res}^{(modes)}) \quad \text{.....} \quad \text{if linear state of stress} \tag{5}$$

$$= (1/f_{\mathrm{Re}s}^{\perp\sigma})^{\dot{m}} + (1/f_{\mathrm{Re}s}^{\perp\parallel})^{\dot{m}} + (1/f_{\mathrm{Re}s}^{\perp\tau})^{\dot{m}} + (1/f_{\mathrm{Re}s}^{\parallel\sigma})^{\dot{m}} + (1/f_{\mathrm{Re}s}^{\parallel\tau})^{\dot{m}},$$

wherein $\dot{m}$ is the mode interaction coefficient (rounding-off exponent, the size of which is high in case of low scatter and vice versa). As a simplifying *assumption,* $\dot{m}$ is given here the same value, regardless of mode interaction zone! The value of $\dot{m}$ is obtained by experience. The author's experience suggests that $\dot{m} = \pi$ is often appropriate.

If a unidirectional fracture stress (i.e. the strength value $\overline{R}_{\perp}^{t}$) is inserted into the equation above, then a point on a 2D- or 3D-failure curve or failure surface (initial or final), described by $f_{\mathrm{Re}s}^{(res)} = 1$, is achieved.

Rounding-off in mode interaction zones of adjacent *mode failure curves* (*partial* failure surfaces) in their interaction zone is leading again to a *global* failure curve (surface), or –in other words-, to a 'single surface failure description' (such as with Tsai/Wu [11], however without its well-known shortcomings)

Note: In practice only 3 modes of the possible 5 ones will interact. However, all modes are included in Eq.(5) in order to have one equation in the numerical analysis, only. If an $f_{\mathrm{Re}s}^{(\mathrm{mod}e)}$ becomes negative, caused by the numerically advantageous automatic insertion (regardless of the sign of the stress) of the FEM stress output $\{\sigma\}=(\sigma_1,\sigma_2,\sigma_3,\tau_{23},\tau_{13},\tau_{12})^T$ into *all* 5 failure conditions, a value of *100* shall replace the negative value. A query serves to exclude these negative value results, for example, if a positive σ_1 is inserted into Eqn(4b).

3. Non-linear Analysis of Lamina and Laminate

3.1 Lamina

-*Hardening:* The degree of non-linearity essentially depends on the non-linear behaviour of the matrix material that manifests itself in the values of $E_{\perp}^{c}$ and $G_{\parallel\perp}$. For the non-linear stress analysis the secant moduli to be applied are derived from the Ramberg/Osgood equation

$$\varepsilon = \sigma / E_{(o)} + 0.002(\sigma / \overline{R}_{p0.2})^{n}. \tag{6}$$

Eq.(6) describes the non-linear stress-strain data very well for the materials analysed here ($E_{(o)}$ is the initial modulus). The so-called Ramberg/Osgood exponent

$$n = \ell n\left(\varepsilon_{pl}(\overline{R}_m)\right) / \ell n\left(\overline{R}_m / \overline{R}_{p0.2}\right) \tag{7}$$

is estimated from the strength point $\left(\overline{R}_m, \varepsilon_{pl}(\overline{R}_m)\right)$ in *Fig.5*, where $\overline{R}_m \Rightarrow \overline{R}_{\perp}^{t}$.

- *Softening:* Beyond *Initial Failure* (IFF), an appropriate progressive failure analysis has to be employed. Often, this softening process is termed as *Successive Degradation Modelling* of *Post Initial*

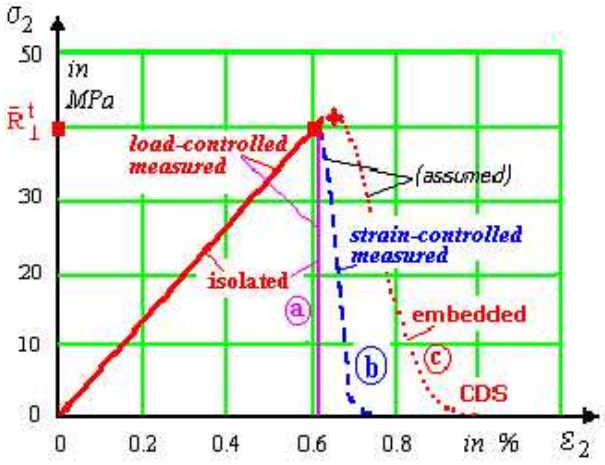

Fig. 5: The differences in the stress-strain behaviour of isolated and embedded UD-laminae. CDS := critical damage state. For the (b)- and (c)-curve Eq(5) is applied. The softening parameters for (b) and (c) are different. Curve (c) = sudden death model.

Due to embedding, point + is higher than the load-controlled strength value ■! Curves (b) and (c) indicate the decaying strength $\overline{R}_{\perp}^{t}(\varepsilon_{\perp}^{t})$ in the softening domain.

failure. This can be performed best by using a failure mode condition that indicates failure type and danger of damage of the material (*material* level) predicted by the size of the stress effort.

Fig. 5 depicts the hardening and the softening curve for a unidirectional lamina. The strain-controlled softening curve has to be assumed here due to the lack of experimental data.
Modelling of *Post Initial Failure* behaviour of a laminate requires that assumptions be made regarding the decaying elastic properties of the degrading, embedded lamina (curve c in *Fig.5*. $E_{\perp}^{c}$ and $G_{\parallel\perp}$ are decreased gradually rather than being suddenly annihilated. A rapid collapse (often named 'ply discount method') of $E_{\perp}^{t}$ is unrealistic and, furthermore, could lead to convergence problems in numeric analysis. A simple exponential function was used to map this softening

$$\sigma_s = \overline{R}_m /(1+\exp[(a_s+\varepsilon)/b_s]), \tag{8}$$

in which suffix s denotes softening. The two curve parameters a_s, b_s are usually estimated from the data of at least two calibration points in achieving a reasonable fit, e.g.

$$(\overline{R}_m,\ \varepsilon\ (\overline{R}_m)) \quad \text{and} \quad (\overline{R}_m \cdot 0.1,\ \varepsilon\ (\overline{R}_m \cdot 0.1)) \tag{9}$$

or another set, as applicable. $\overline{R}_m$ corresponds generally to the strength of the isolated lamina under uni-axial loading. Eq.8 models the softening part of the stress-strain curve of a lamina which is embedded in a laminate, and thus, it includes the effect of the altering micro-crack density up to a critical damage state (CDS), [13, 8]. Curve c is therefore termed an *effective* curve.

Application of an effective stress-strain curve: Due to the 'in-situ' strength effect, the author regards the peak value of the *effective* stress-strain curve of an embedded lamina to be slightly higher than the strength value $\overline{R}_m$ of an *isolated* lamina. Reason is the change from the 'weakest link behaviour' to the real redundant behaviour of a laminate. However, due to a lack of knowledge and for the sake of simplicity, this 'peak value' is lowered down to the mean strength $\overline{R}_m$ in the analytical description of softening. Due to mapping reasons, e.g. for the mode $F_{\perp}^{\sigma}$ 0.99 $\overline{R}_{\perp\parallel}$ was taken instead of $\overline{R}_{\perp}^{t}$ ($\equiv \overline{R}_m$) as the calibration point for the softening curve (see also sub-section 3.2).

Determination of the Degrading Elasticity Properties of the Lamina: By employing the equivalent stress reached in each failure mode the associated secant modulus of each mode was determined for the hardening and the softening regime. Considering a consistent stress concept for all $\sigma_{eq}^{(mod\,es)}$ an *explicit* dependency $E_{sec}(\sigma_{eq}^{(mod\,e)})$ has to be provided. For reasons of achieving such an

explicit formulation two separate formulae are discriminated which are linked (Eq.(9)) in the strength point. This automatically respects that the chosen non-linear calculation procedure demands the dependen-ces of the secant moduli on the corresponding equivalent stress. These dependences are (see *Fig. 5*), e.g. for $F_{\perp}^{\tau}$:

- Pre-IFF analysis of lamina : $\Delta\sigma > 0$ (*increasing stress, hardening*) from Eq.6

$$E^{c}_{\perp(\sec)} = E^{c}_{\perp(o)} / [1+0.002\cdot(E^{c}_{\perp(o)} / R^{\perp c}_{p0.2}) \cdot (\sigma^{\perp\tau}_{eq} / R^{\perp c}_{p0.2})^{n^{c}_{\perp}-1}] \qquad (9)$$

- Post-IFF analysis of lamina : $\Delta\sigma < 0$ (*decreasing stress, softening*) from Eq.8

$$E^{t}_{\perp(\sec)} = \sigma^{\perp\sigma}_{eq} / \varepsilon(\sigma^{\perp\sigma}_{eq}) = (\sigma^{\perp\sigma}_{eq} / b^{\perp t}_{s}) / \left[\ell n\left(\frac{R^{t}_{\perp} - \sigma^{\perp\sigma}_{eq}}{\sigma^{\perp\sigma}_{eq}}\right) - \frac{a^{\perp t}_{s}}{b^{\perp t}_{s}} \right] \qquad (10)$$

For the other modes the same formula is valid, however, the mode parameters are different.

3.2 Laminate

The solution procedure of the non-linear analysis aims to establish static equilibrium at each load step after material properties have been changed. For each iteration the procedure is repeated until convergence (equilibrium) is reached or total failure. A correction of the fibre angle in accordance with the change of the specimen's geometry as consequence of large strain behaviour has been considered. In the MATHCAD-based code 'CLT FRP Non-linear', generated in [8, 15] for the Failure Exercise, the self-correcting secant modulus method was applied to describe the successive degradation. The laminate's stiffness matrix is recomputed after each step. Then, the stresses σ_2 and τ_{21} in the laminae of the laminate are computed by using secant moduli from the $\sigma_2(\varepsilon_2)$- and $\tau_{21}(\gamma_{21})$-stress/strain curves and from them the equivalent stresses are determined.

In the non-linear computations for a small load increment, sometimes just one iteration step is needed in a secant modulus procedure in order to roughly consider stress-redistribution, that means, load from the weakening matrix (matrix-dominated modes) is transferred to a fibre (fibre mode). After having reached $f^{(res)}_{\mathrm{Re}\,s} = 1$, this value *1* is kept as maximum value in the further degradation procedure which causes a stress redistribution towards the fibres as far as the fibre net allows it. Thereby, also the residual stresses are reduced similar to the situation with metallic materials where increasing non-linearity reduces stiffness, and the residual stresses.

4. Application to the UD Lamina Test Cases of the Failure Exercise (see [14])

In this first test case (*Fig.6*), the blindly predicted failure envelope through the given strength values

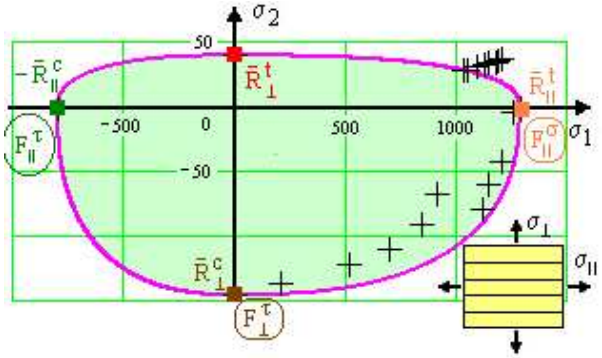

Fig.6: Biaxial fail. stress envelope ($\sigma_{2,}, \sigma_{1}$) in MPa. UD-lamina. E-glass/MY750epoxy. Eq.(1). Hoop wound tube data +, $\dot{m} = \pi$. $\sigma_1 = \sigma_{hoop}$, $\sigma_2 = \sigma_{axial}$ Provided: $\{\bar{R}\} = (1280,\ 800,\ 40,\ 145,\ 73)^T$, Eqs.(2, 5), $b_{\perp\parallel} = 0.13$. Refs[4, 5],

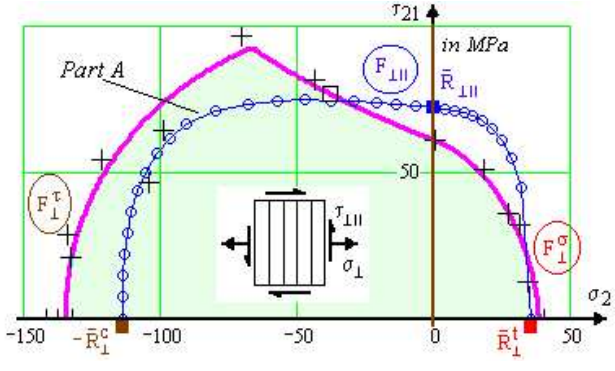

Fig. 7: 'Blind' data: $b_{\perp\parallel} = 0.13$, $\dot{m} = \pi$ *assumed,* $\{\bar{R}\} = (1140,\ 570,\ 35,\ 114,\ 72)^T$ provided. Eq.(5) Assumed 'best fit data set': $\dot{m} = 2.1$, $b_{\perp\parallel} = 0.56$, $\{\bar{R}\} = (1140,\ 570,\ 38,\ 135,\ 62)^T$. ($1 \equiv \parallel$, $2 \equiv \perp$). *MaxTau =105 MPa, [14], Annex I.*

does not map the provided test data satisfactorily due to 'jumping' of measured data in the fourth quadrant.
The prediction in *Fig.7* (circles) primarily does not match because the strength data given do not fit to the given measured values (crosses). Besides this the parameter $b_{\perp\parallel}$ could not be determined in advance. Second point is the peak point (never seen in the various experiments of MAN and of literature). Despite assuming this value is not correctly measured the cross curve was mapped with the result: The FMC failure criterion can map this test case with an associated parameter set.
As the test data provided for *Fig.7* in the negative domain are not typical, own test results (*Fig.7*) will be given in Chapter 6.2. For other cross-sections of the multi-dimensional failure surface, see Ref[8].

5. Application to the 4 UD Lamina-composed Laminate Test Cases of the Failure Exercise

Most engineers assume that FF in at least one lamina of a laminate means final failure of the laminate. Therefore, the biaxial failure envelopes for final failure of laminates predicted by the various authors do not differ that much, as long as the laminates are 'well-designed and have three or more fibre directions. The 'strengths' of these laminates are 'fibre dominated'. Also, the predicted stress-strain curves of such laminates look very similar because the fibres being much stiffer than the matrix carry almost the full loads. Different degradation procedures after the onset of inter-fibre failure (IFF) do therefore not influence the predicted strains very much. This is especially true for CFRP laminates.

5.1 Failure Curves (see [14])

In the following figures the fracture initiating modes together with the actual lamina is marked.
In *Fig.8* the mapping result is satisfying except for the negative domain. The compression strength (not correctly provided) had to be corrected by the author. This helped to reduce the gap to the prediction values. Probable further explanations could not be drawn from test description [4, 5].
In the next test case, illustrated by *Fig.9*, mapping quality was not sufficient on the y-axis. In the third towards fourth quadrant buckling failure replaces the strength failures addressed in the Failure Exercise, only.
Fig.10 shows high scatter on the negative $\hat{\sigma}_x$ axis. Again of course, buckling failure cannot be mapped. An estimated rounding by considering joint failure probability of adjacent laminae is exemplarily depicted in this figure.
In *Fig.11* high discrepancies are recognized on the positive $\hat{\sigma}_y$ axis. The deviation in the third quadrant is extreme. However, it might be explained, see [14], by the fact that the lay-up is not too wedge failure critical. Regarding this point, respecting the 3D-stress state and a specific speculation on a probable stabilizing effect on the inner surface the predicted values may be corrected up to the level (-800,-400).

5.2 Laminate Stress-Strain Curves (see [14])

According to usual stiffness requirements, in order to guarantee the functionality of the structural product, limitations are always given. So, some test cases are more chosen to investigate the *limits of theory* not just the practical regime.

Fig.12 and *Fig.15* outline that the non-linear coding utilized here came to its limits when reaching the higher strains.
In *Fig.13*, although it is the well-designed test case 'pressure vessel', the highest discrepancy is given. Furthermore, due to symmetry, theory demands for two parallel curves. This is not measured and evaluated . Why? As the readings of the strain gauges are affected by the end conditions, which caused barrelling, plane CLT analysis is at its limit. It would need a Finite Element Analysis. However, because at fracture netting theory is applicable in this 'netting theory-designed laminate',

a correction can be performed utilizing netting theory and the measured fracture strains. This leads to an estimation of the higher fracture loading shown in the figure.

The *Figures 14, 16, 17* confirm that the stress-strain curve of the usually well-designed laminates

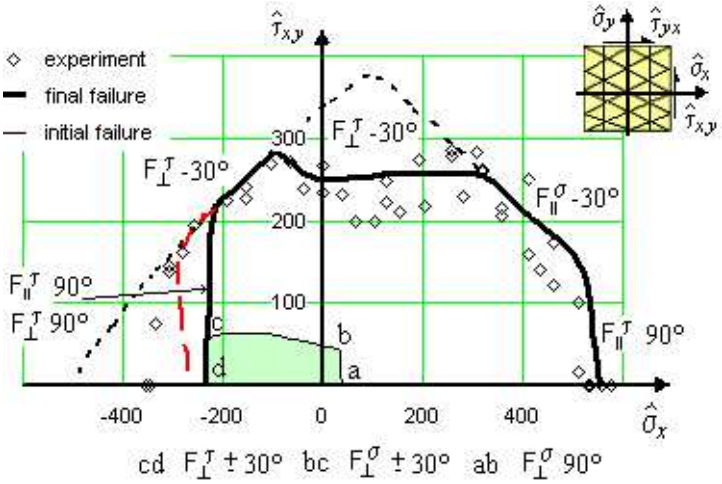

Fig.8: Initial and final biaxial failure envelope $\hat{\tau}_{xy}(\hat{\sigma}_x)$. $[90/+30/-30]_n$ -laminate. E-glass/LY556 epoxy. $\hat{\sigma}_x$ is parallel to 0°-direction. ΔT= -68°C. $\{\overline{R}\} = (1140,\ 570,\ 35,\ 114,\ 72)^T$, test data provided. $b_\perp^\tau = 1.09$, $b_{\perp\parallel} = 0.13$, $\dot{m} = \pi$. Dashed line: increase due to $\overline{R}_\perp^c = 114 \Rightarrow 138 MPa$, error in data provision.

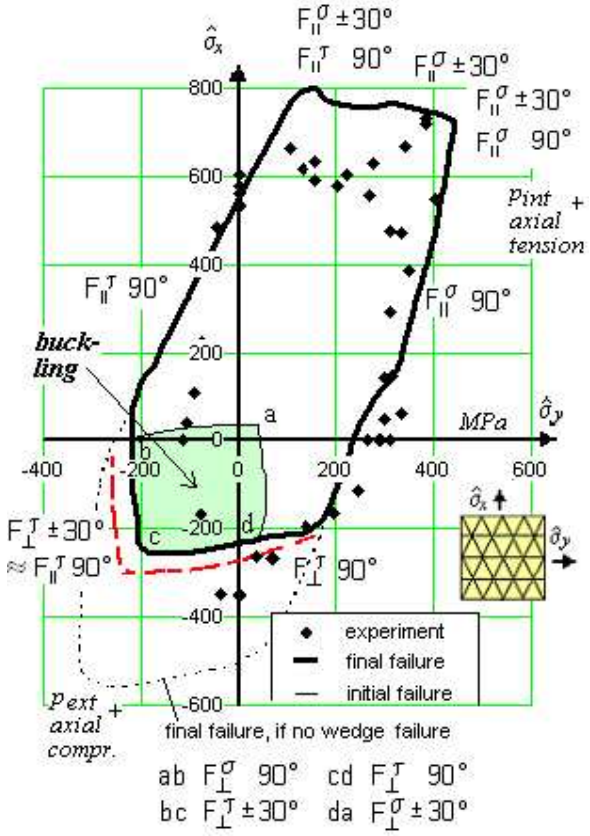

Fig. 9: Initial and final biaxial failure envelopes $\hat{\sigma}_y(\hat{\sigma}_x)$. $[90/+30/-30]_n$-laminate (n varies between 1 and 4). E-glass/LY556 epoxy. ΔT= -68°C. Tube Test data provided. $b_\perp^\tau = 1.09$, $b_{\perp\parallel} = 0.13$, $\dot{m} = \pi$.

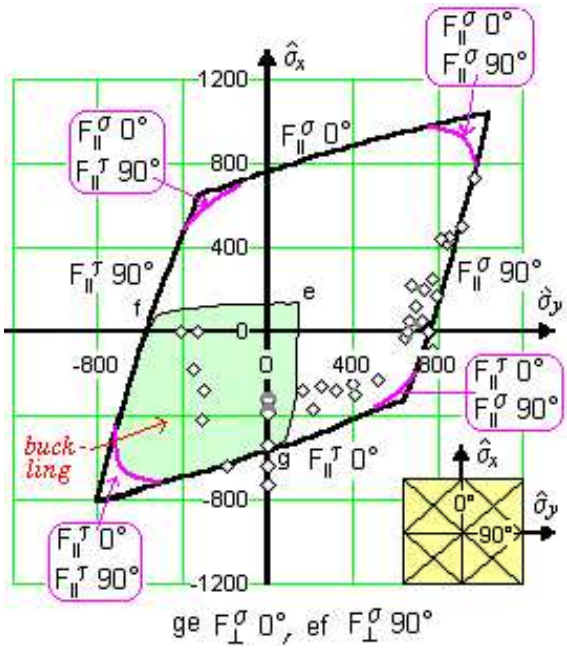

Fig. 10: Initial and final failure envel. $\hat{\sigma}_y(\hat{\sigma}_x)$ in MPa. $[0/45/-45/90]_s$-laminate, AS4/3501-6. $\hat{\sigma}_y$: = average hoop stress of the laminate, x:=0° direction. ΔT= -125°C. Hand lay-up cylinder. $b_\perp^\tau = 1.09$, $b_{\perp\parallel} = 0.13$, $\dot{m} = \pi.1$. $\{\overline{R}\} = (1950,\ 1480,\ 48,\ 200,\ 79)^T$.

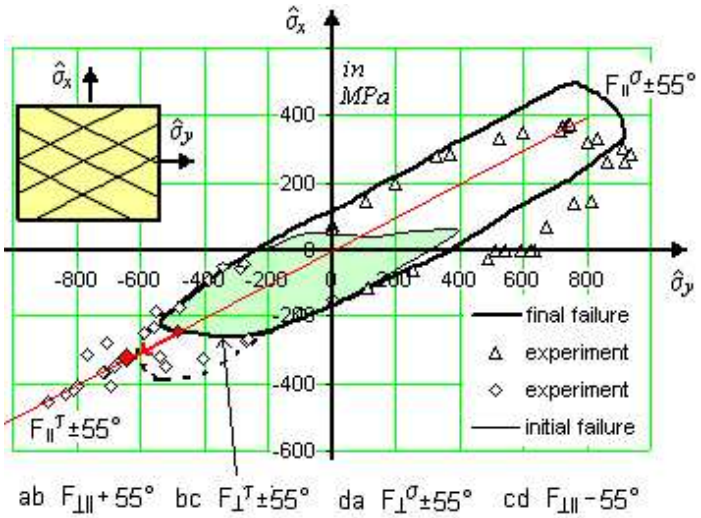

Fig. 11: Initial and final failure envelope $\hat{\sigma}_y(\hat{\sigma}_x)$. [+55/-55/55/-55]-laminate, E-glass/MY750 epoxy. Filament wound tube test data. ◆ corrected value. ΔT= -68°C. Limit of usage (lou) at γ = 10 %. Dashed curve: final failure of a full 'wedge failure'-insensitive stack.

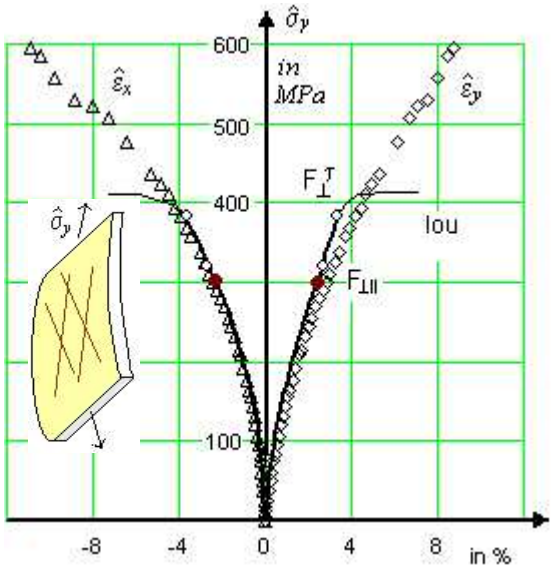

Fig 12: Stress-strain curves for $\hat{\sigma}_y$: $\hat{\sigma}_x$ =1:0 *(radial loading by p_{int} + axial compression load).* Tube. [+55/-55/55/-55] -laminate, E-glass/MY750 ; ΔT= -68°C. y:=hoop direction. $\hat{\sigma}_y = \sigma_{hoop}$. Final blind prediction point● *max*γ= *10 %.*

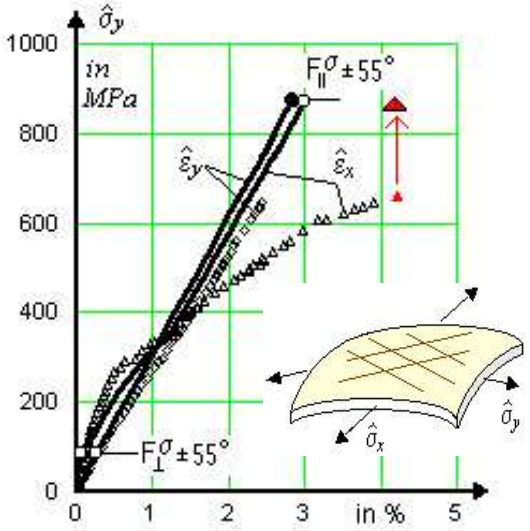

Fig. 13: Stress-strain curves for $\hat{\sigma}_y$: $\hat{\sigma}_x$ = 2:1 *(p_{int}),* [+55/-55/55/-55]-laminate. E-glass/ MY750 .ΔT= -68°C. Corrected maximum test values. Final blind prediction point ●.

$\hat{\sigma}_y = \sigma_{hoop}$

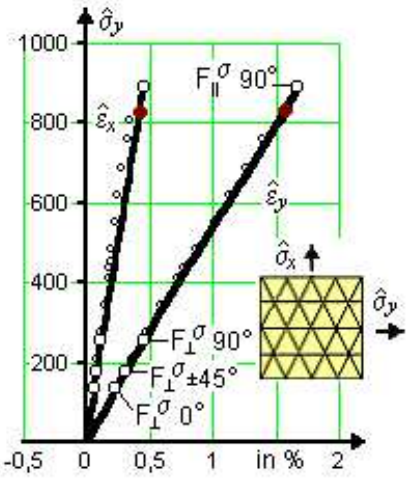

Fig. 14: Stress-strain curves for $\hat{\sigma}_y$:$\hat{\sigma}_x$ = 2:1 *(p_{int}).* [0/+45/-45/90]$_s$-laminate. AS4/3501-6 epoxy. ΔT= -125°C. Final blind prediction ●.

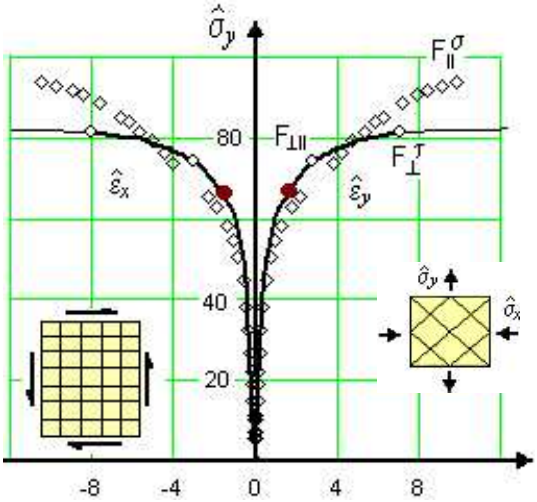

Fig. 15: Stress-strain curves for $\hat{\sigma}_y$:$\hat{\sigma}_x$ = 1:-1 *(shear by p_{int} + axial compression)* .[+45/-45/45/-45]-laminate. E-glass/MY750. ΔT = -68°C. Bulging reported in experiment. $\hat{\sigma}_y = \sigma_{hoop}$.

can be predicted pretty well. In *Fig.17* the 'blind' prediction was the same value lower than the measured value as the final one (coding 'improved', failure criteria (4d,e) simplified) was higher.

The influence of the IFF criteria reduces with increasing degradation. This effect is comparable to the residual stress influence.

6 Remarks on Test Specimens and Evaluation of Experimental Results

6.1 Effects to be considered

If applying test data from tensile coupons of isolated laminae to a lamina embedded in a laminate, one has to consider that tensile coupon tests deliver test results of *weakest link type* (series model, see [14]). However, an embedded lamina or even a lamina constrained on only one surface side, belongs to the class of *redundant type behaviour* (parallel spring model). Due to being strain-

controlled, the material flaws in a *thin* lamina cannot grow freely up to micro-crack size in the thickness direction (this is called *thin layer effect*), because the neighbouring laminae act as micro-crack-stoppers. In addition to reasons regarding fracture mechanics, the strain energy release rate

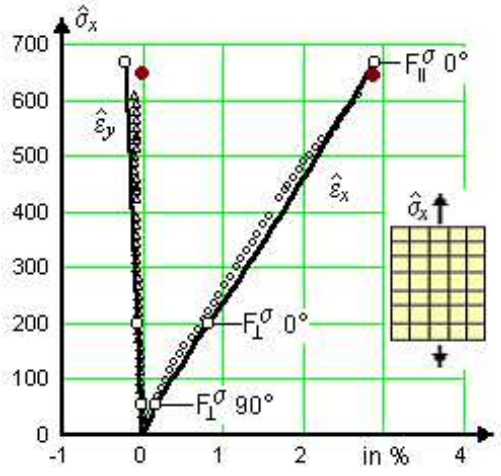

Fig. 16: Stress-strain curves for $\hat{\sigma}_y$:$\hat{\sigma}_x$ =0:1, *(axial tension).* [0/90]$_s$-laminate. Coupon!. E-glass/ MY750. ΔT= -68°C. Final blind prediction point●.

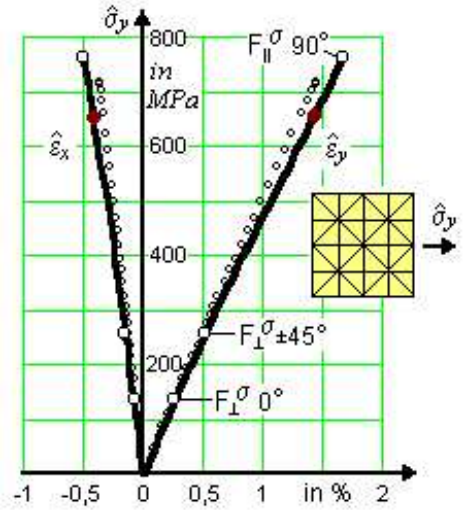

Fig. 17: Stress-strain curves for $\hat{\sigma}_y$:$\hat{\sigma}_x$ =1:0. *(radial loading induced by* p_{int} + *axial compression).* $\hat{\sigma}_y = \sigma_{hoop}$ [0/+45/-45/90]$_s$-laminate. AS4/3501-6 epoxy.. ΔT=-125°C.

responsible for the development of damage in the 90° plies from flaws into micro-cracks, increases with increasing ply thickness. Therefore, the actual absolute thickness of a lamina in a laminate is a driving parameter for the initiation or onset of micro-cracks.

6.2 Evaluation Errors

A correct analysis of boundary conditions and stress state of the test specimen is mandatory before evaluating and applying the data. In this sense, tubes instead of the flat coupon specimens will help to avoid problems associated with the 'free edge effect'. A wide range of bi-axial stresses can be achieved. Real tri-axial stress states require refined specimens (see [9] page 107 and [14]). Tubular specimens may be subjected to internal and external pressure, to torsion and axial forces. But, even tube testing is not free of problems such as barrelling (bulging), caused by end constraints, or buckling (is not a *strength* failure mode) of the cylinder. Further, tubes may exhibit non-linear changes in geometry during loading (widening). Therefore, a non-linear analysis has to take into account both, large strains *and* large deformations. If these facts are not considered in test evaluation *and* in analysis one has compared apples and oranges. Also in the Failure Exercise, the plane CLT evaluation of un-deformed specimen geometry induced more or less essential errors.

The next two figures shall outline some typical errors we might cause when evaluating test results without the high carefulness needed.
In *Fig.18* the test curves should lie on top of one another due to the symmetric geometry and due to loading. Different curves for $\hat{\varepsilon}_x$ and $\hat{\varepsilon}_y$ indicate bulging, however. Hence we should check the evaluation of the test results: At fracture -according to micro-crack spacing- netting theory can be applied to assess the test data of this well-designed laminate. Input of the simple computation is: $\varepsilon_x^{fracture} = 2.18\%$, $\varepsilon_y^{fracture} = 2.48\%$ and $\sigma_{\perp} = \tau_{\perp\|} = 0$ due to zero matrix stiffness. With these values *at first* the maximum *experimental* strength of 430 MPa is *increased* (arrow) to $\hat{\sigma}_x = \hat{\sigma}_y = 530$ *MPa. Secondly,* a lower effective tensile strength $\sigma_{\|}^{t} = 1062$ *MPa* is derived. And from this, the maximum *theoretical* fracture stress according to the effective fracture strength values is *reduced* down to a value $\hat{\sigma}_y$ = *660x(1062 /1280) MPa=547 MPa*, with *1280 MPa* the given too high tensile

strength. The twofold $F_{\parallel}^{\sigma}$ failure in both 45° layers will reduce the theoretical fracture value a little more. Experimental and theoretical curves coincide now.

Fig.19 shows the experimental (τ_{21}, σ_2) results obtained from tests on unidirectional carbon-fibre reinforced epoxy tubes superimposed on *the blind* predictions. In this case, the loading of this *axially* wound tube is torsion with internal pressure plus axial loading. The test data, delivered by different test specimens, show wide scatter and 'jumping' in the positive domain. As this tube is heavily shearing under torsional loading the data given might not be the searched lamina stresses $(\tau_{\perp\parallel}, \sigma_{\parallel})$ but stresses belonging to the structure coordinate system (x,y). Therefore, an attempt is made to re-evaluate the experimental data (in *MPa*) due to: At first one determines the shear angle γ by non-linear CLT analysis and secondly one transforms the stress data provided into the real (||-$\perp$) coordinate system of the lamina. The computation delivers the real lamina stresses, as follows:

$\sigma_{\parallel} = \sigma_x (\cos\gamma)^2 + 2\tau_{yx} \cos\gamma \sin\gamma$, $\sigma_{\perp} = \sigma_x (\sin\gamma)^2 - 2\tau_{yx} \cos\gamma \sin\gamma$, $\tau_{\perp\parallel} = -0.5\sigma_x \sin 2\gamma + \tau_{yx} \cos 2\gamma$, e.g.

$(\sigma_x \equiv \sigma_1,\ \sigma_y \equiv \sigma_2,\ \tau_{yx} \equiv \tau_{21}) = (1000, 0, 123),\ \gamma = +3° \Rightarrow (\sigma_{\parallel}, \sigma_{\perp}, \tau_{\perp\parallel}) = (1010, -10, 70).$

The angles 3° and –2° result in size and sign from the above described CLT computation that uses the corresponding set of combined fracture stresses given. The finding is: Both corrected test points practically fall on the mapped curve. Discrepancy is vanished!

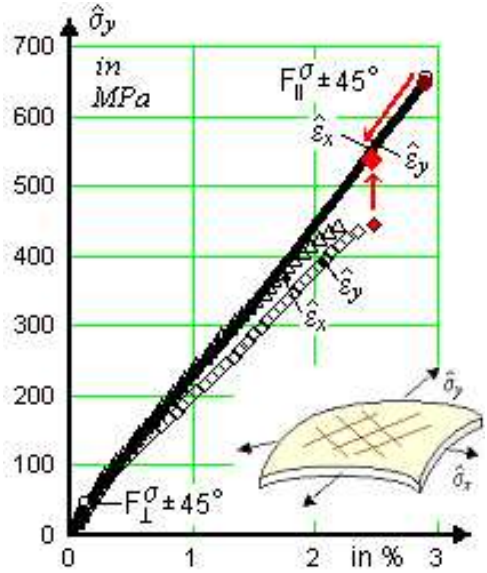

Fig. 18: Stress-strain curves for $\hat{\sigma}_y : \hat{\sigma}_x = 1:1$, *($p_{int}$ + axial tension).* [+45/-45/45/-45]-laminate. E-glass/MY750. ΔT= -68°C. Bulging reported in experiment. $\hat{\sigma}_y = \sigma_{hoop}$ ◆ maximum test value after correction. Final blind prediction point●.
$\{\bar{R}\} = (1280,\ 800,\ 40,\ 145,\ 73)^T$.

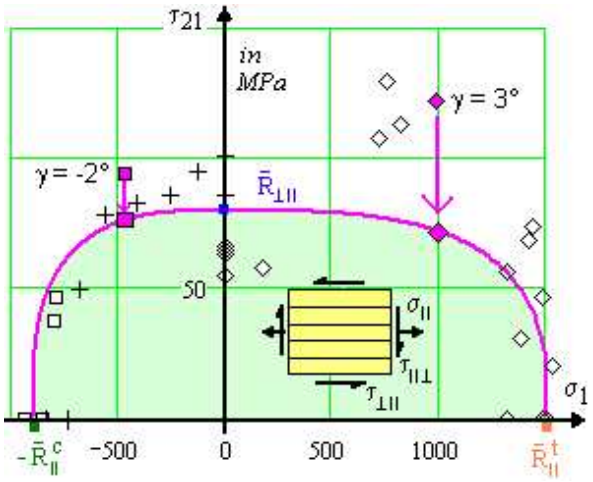

Fig. 19: Biaxial failure stress envelope (τ_{21}, σ_1) in MPa. UD-lamina T300/BSL914C epoxy. Axially! wound Tube. $\{\bar{R}\} = (1500,\ 900,\ 27,\ 200,\ 80)^T$.
$\dot{m} = \pi$ Corrected test data due to computed shear deformation γ ■◆ : Transformation of $(\sigma_1, \sigma_2, \tau_{21})$ into real lamina stresses $(\sigma_{\parallel}, \sigma_{\perp}, \tau_{\perp\parallel})$

The quality of theory and non-linear coding in managing the load transfer from matrix to the fibres determines the quality of the analytical results. However, as practice requires well-designed laminates analysis becomes not that non-linear in real life.

Eventually, in *Fig.20* the indicated own experimental data is presented to proof that the peak data in the negative (τ_{21}, σ_2)domain -this is the main IFF failure curve- are questionable.

7 Summary

7.1 Lessons Learned

7.1.1 Theory

• The UD fracture conditions employed in the theory are proven to work in practice. The full capacity of the 3D-fracture criteria could not be fully verified. Some essential stress combinations

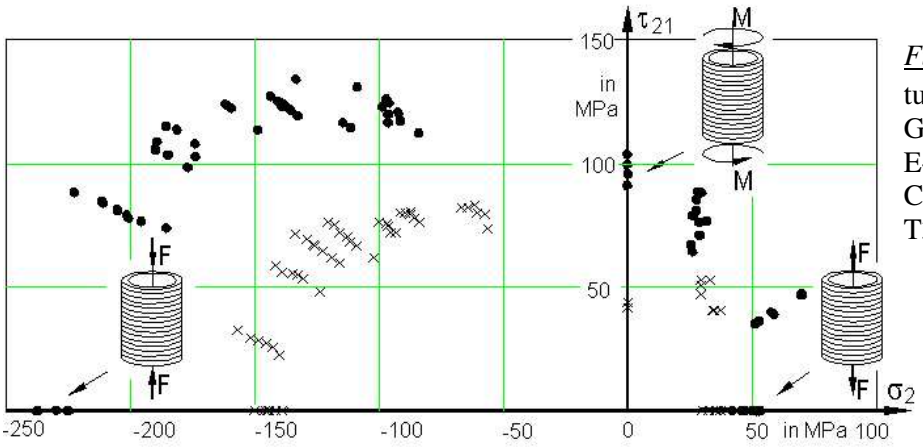

Fig20: (σ_2, τ_{21})-IFF curves, tubes [10].
GFRP:
E-lass/LY556/T976/DY070
CFRP:
T300/LY556/HT976

are still not tested. As the organizers could not provide sufficient information on the IFF modes it was not possible to confirm the accuracy of all predicted IFF values.

• In the matrix-dominated load cases the IFF (respecting degrading lamina strength) have a strong influence on the stress-strain behaviour. *Final failure* occurs after the structure has degraded to a level where it is no longer capable of carrying additional load. This is most often caused by FF, however in specific cases by an IFF, too. An inclined wedge-shaped inter-fibre crack caused by $F_{\perp}^{\tau}$ can lead to final failure if it damages the neighbouring layers by its capability to cause 3D states of stress and eventually delamination.

• In case of large strains the non-linear analysis has to be further improved

• In composite laminates composed of stiff fibres and well-designed by netting theory the fibre net controls the strain behaviour. Here, predictions are practically fully satisfying in the frame of the scatter of the design parameters

7.1.2 Comparison Theory-Test including Testing

The predicted initial and final failure envelopes did not match the test results in a number of instances. Theory was expected to give the largest discrepancy with test data in the high shear area because the computer software code developed in the present work for non-linear analysis requires further work to eliminate any convergence problems in case of high shear strains.
However, high shear strains in practice are seldom permitted and do not occur in well-designed laminates. In case of the not well-designed laminates we have to ask ourselves: What is failure? A 'limit of deformation' or 'limit of usage', is to be defined there as a functional limit.

All sources that may lead to discrepancy between prediction and test are listed now:
* Errors and approximations in the theory
* Errors in the given material properties
* Errors in the experimental results
* Errors in the evaluation of the experiment and interpretation of data
* Differences between fabricated and analysed laminate model
* Lack of test data.

When developing and testing a laminated structure -in order to understand remaining gaps between theory and experiment- we have to keep in mind:
- Experimental results can be far away from the reality like a bad theoretical model
- Theory 'only' creates a model of the reality, experiment is 'just' one realisation of the reality
- Usually a laminate is designed to be stable as a truss (netting theory applicable), and the laminae are stacked at angles to generate a laminate robust against possible load changes. This procedure

leads to a well-designed laminate.

7.2 Outlook

•Industry seeks to replace the expensive 'Make and Test' design method by verified and benchmarked predictive tools that engineers could use with confidence. A practical FEA-based 'progressive failure analysis procedure' has to be provided to designers. An implementation into a FE code is expected to provide a widely accepted design tool

•Industry also has to cope with damage and the Proof of Design (justification) of damaged laminates. Practical criteria for the assessment of damage size and criticality of delamination are needed. Sufficiently well working NDI methods for damage detection are desired in order to avoid *un-stable* (sudden) delamination fracture. A design guideline for improving damage tolerance analysis has to be provided. Further, the treatment of fatigue and *stable* damage growth has to be enhanced and may be better enhanced on failure mode basis

•Author's main assessments for UD laminates and textile laminates are:

-3D-*stress* analysis of laminated shells obtained by commercial FEA codes (MARC, NASTRAN etc) is not adequate. It is still too time-consuming and pre-processing does not inform about design driving modes as well as reserve factors, [8], demanded for the 'Proof of Design'. Here, an improvement is highly appreciated

-There is still a need for generating reliable multi-axial test data (not all section planes of the multi-axial fracture body are verified as one may conclude from the *Figures 5,6,7*). This could be achieved through a coordinated and collaborative test research programme between leading research institutions. Other areas include the development of probabilistic models and the encouragement of an improved worldwide standardization where manufacturers, technical associations and authorities are all involved

- As the area 'in-situ behaviour of the embedded laminae' has not attracted much attention further work is highly recommended. Therefore, for a better characterisation of post failure behaviour, the softening curves have to be provided.

-Verification of engineering approaches, based on a qualified FEA-output level when analysing the test specimen, is necessary. There is surely a lot open in failure analysis of UD-stacked laminates but one should not forget: The textiles are waiting. And, one first needs the certification in order to begin the production of structural parts made from textiles

- Smeared modelling of a UD material (consists of fibres and matrix) comes to a limit in the mode $F_{\parallel}^{\sigma}$. Failure occurs when the fibre strength σ_{1f} is reached. The failure formulation considers this situation by utilizing the strain.

• Regarding the theoretical and experimental investigations carried out in Germany on the *lamina* material level in recent years (and are still going on, e.g. [16]) the understanding has improved greatly and seems to be a good basis to tackle *laminates* made up of UD-laminae or fabric laminae etc.
Multi-axial tape lay-ups with low stitching density by the binding threads in z direction of the laminate can be approximately treated by the UD FMC model.
For 'higher textile pre-forms' (woven fabrics, 3D, heavily stitched laminates, etc.) *engineering models* have to be developed. The work in this field has been initiated.E.g. the author's first steps indicate that the transferability to fabrics (rhombically-orthotropic) composites should work

• Initial failure stresses are very important where a standard requires a Proof of Design to IFF. This means: if at $DLL \cdot j_{yield}$ level no IFF is permitted. For the higher *Ultimate Proof of Design*, in case of a well-designed laminate, initial failure prediction has not that much importance.

In any case, the comparisons between theoretical predictions and the experimental data helped to identify certain areas where further theoretical and experimental work is required for a final verification of theory, at least for achieving a better understanding of failure prediction.
These include: 1.) Obtaining more representative experimental UD data to really make a judgement of the UD criteria possible.2.) Improving non-linear laminate analysis: placing greater emphasis on

the strain-controlled behaviour of an embedded lamina, and improving the computational capabilities of the generated computer code including modelling of material and geometrical non-linearities. 3.) Enhancing in future tests an information gain on IFF occurrence in experiment.

7.3 Compliance with FDM 03 Conference

• Aims of Conference "Promotion of further international co-operation among scientists and practising engineers": On the way since 10 years.

• Objectives of Conference" Production of Integrated Approach to problems of Fracture Failure, Fatigue and Safe Design": Cooperation of all disciplines of the conference fields is automatically enhanced if looking (mandatory) over the 'material fences'. Synergy is increased then.

Acknowledgement: Many, many thanks to the referees and, especially, to the organisers of these 'Olympic Games on static strength criteria for composites'. This was an enormous effort you had to spend Mike, Peter and Sam. During this mammoth task over 11 years you never gave up! Excellent.

References

[1] *Failure Criteria of fibre-reinforced-polymer Composites* (Part B of the Failure Exercise). Composites Science and Technology 62 (2002), 12-13, 1479-1797

[2] Part C of the Failure Exercise, Composites Science and Technology (in press 2003)

[3] Hinton, M.J. and Soden, P.D.*: Predicting failure in composite laminates: the background to the Exercise.* Composites Science and Technology 58 (1998), 7, pp. 1001-1010

[4] Soden, P.D., Hinton, M.J. and Kaddour, A.S.: *Lamina Properties, Lay-up Configurations and loading conditions for a Range of Fibre-reinforced Composite Laminates*. Special Issue, Composite Science and Technology 58 (1998), 1011-1022

[5] Soden, P. D., Hinton, M. J. and Kaddour, A. S.: *Experimental failure stresses and deformations for a range of composite laminates subjected to uniaxial and biaxial loads*. Composites Science and Technology 63 (2003)

[6] Hinton, M. J., Kaddour, A. S. and Soden, P. D.: *A Comparison of the Predictive Capabilities of Current Failure Theories for Composite Laminated, Judged against Experimental Evidence*. Composite Science and Technology 62 (2002), 1725-1797

[7] Guidelines 728 JET, DORNIER Luftfahrt GmbH: *Structural Analysis and Certification Documentation*

[8] Cuntze, R G and A. Freund: *The Predictive Capability of Failure Mode Concept-based Strength Criteria for Multidirectional Laminates. Part A.* Composites Science and Technology, (ready for press)

[9] Puck, A. and Schürmann, H.: *Failure Analysis of FRP Laminates by Means of Physically based Phenomenological Models.* Composites Science and Technology 62 (2002), 1633-1662

[10] Cuntze, R.G., Deska, R., Szelinski, B., Jeltsch-Fricker, R., Meckbach,S., Huybrechts, D., Kopp, J., Kroll, L., Gollwitzer, S., and Rackwitz, R.: *Neue Bruchkriterien und Festigkeitsnachweise für unidirektionalen Faserkunststoffverbund unter mehrachsiger Beanspruchung –Modellbildung und Experimente–.* VDI-Fortschrittbericht, Reihe 5, Nr. 506 (1997), 250 pages. (*New fracture criteria (Puck's criteria) and Strength 'Proof of Design' for Uni-directional FRPs subjected to Multi-axial States of Stress –Model development and experiments-.* In German)

[11] Tsai, S.W. and Wu, E.M.: *A General Theory of Strength for An-isotropic Materials*. Journal Comp. Materials 5 (1971), 58-80

[12] Rackwitz, R. and Cuntze, R.G.: *System Reliability Aspects in Composite Structures.* Eng.' Opt. 11 (1987), 69-76

[13] Cuntze, R.G.: *Deterministic and Probabilistic Prediction of the Distribution of Inter-Fibre Failure Test Data of Pre-strained CFRP Tubes composed of Thin Layers and loaded by radial pressure*. Wollongong. Advanced Composites '93, 579-585. The Minerals, Metals & Materials Society, 1993

[14] Cuntze, R. G: *The Predictive Capability of Failure Mode Concept-based Strength Criteria for Multidirectional Laminates. Part B*. Composites Science and Technology, (ready for press for Part C edition)

[15] VDI 2014: German Guideline, sheet 3 *'Development of FRP components, Analysis'*.(German and English. In press)

[16] Michaeli, W. and Knops, M.: *Stress and strength analysis of structural components with inter fiber failure.-Experimental and theoretical work-.* Proceedings SAMPE, Long Beach, 12.-16.5.2002.